Makara Journal of Science

Volume 26
Issue 3 *September*

Article 3

9-30-2022

# Modulation of the NF-κB Activation Pathway by Phycocyanobilin from Spirulina platensis: An in Silico Study

Febriana Catur Iswanti
*Department of Biochemistry and Molecular Biology, Faculty of Medicine, Universitas Indonesia, Jakarta 10430, Indonesia*

Hastuti Handayani S Purba
*Master's Programme in Biomedical Sciences Faculty of Medicine, Universitas Indonesia, Jakarta 10430, Indonesia*

Ani Retno Prijanti
*Department of Biochemistry and Molecular Biology, Faculty of Medicine, Universitas Indonesia*

Fadilah Fadilah
*Departement of Medical Chemistry, Faculty of Medicine, Universitas Indonesia,*

Linda Herlina
*Departement of Medical Chemistry, Faculty of Medicine, Universitas Indonesia,*

*See next page for additional authors*

# Modulation of the NF-κB Activation Pathway by Phycocyanobilin from Spirulina platensis: An in Silico Study


## Authors

Febriana Catur Iswanti, Hastuti Handayani S Purba, Ani Retno Prijanti, Fadilah Fadilah, Linda Herlina, and Reni Paramita

Makara Journal of Science, 26/3 (2022), 166–181
doi: 10.7454/mss.v26i3.1377

# Modulation of the NF-κB Activation Pathway by Phycocyanobilin from *Spirulina platensis*: An in Silico Study

Febriana Catur Iswanti[1], Hastuti Handayani S. Purba[2,3], Ani Retno Prijanti[1], Fadilah[4], Linda Erlina[4], and Reni Paramita[1*]

1. Department of Biochemistry and Molecular Biology, Faculty of Medicine, Universitas Indonesia, Jakarta 10430, Indonesia
2. Master's Programme in Biomedical Sciences Faculty of Medicine, Universitas Indonesia, Jakarta 10430, Indonesia
3. National Research and Innovation Agency, Jakarta 10340, Indonesia
4. Departement of Medical Chemistry, Faculty of Medicine, Universitas Indonesia, Jakarta 10430, Indonesia

[*]*E-mail: reni.paramita01@ui.ac.id*

Received July 7, 2022 | Accepted August 26, 2022

## Abstract

Several studies have predicted the molecular interactions of the active ingredient of *Spirulina platensis* as an anti-inflammatory compound. However, these interaction studies did not review the modulation of the NF-κB activation pathway, which involves various factors. This study demonstrated the potential of the bioactive compounds of *S. platensis* for modulating immune function by reducing inflammation through the inhibition of the NF-κB activation pathway. Phycocyanobilin was predicted to have good potential for molecular docking with multisubunit IκB kinase (IKK)1/IKKA, IKK2/IKKB, NF-κB-inducing kinase, and the IκBα/NF-κB complex. Furthermore, β-carotene exhibited good potential for interactions with NF-κB essential modulator/IKK and the NF-κB complex, and α-glucan had the potential for interactions with COX-2. Therefore, supplementation with *S. platensis* and its bioactive compounds is expected to provide optimal benefits.

*Keywords: anti-inflammation, Modulation, NF-κB, phycocyanobilin, S. platensis*

## Introduction

During the last century, breakthroughs in the health and scientific fields have allowed humans to live longer in healthier states [1]. Natural products have become people's choice because of the many disadvantages of drug therapy, including side effects [2, 3]. One nutritional supplement that is rich in available nutrients is *Spirulina platensis*, a blue-green algae that is commonly used as a dietary supplement because of its abundant flavonoid and sulfalipid contents [4, 5]. The biological functions of the bioactive compounds found in *S. platensis* include increasing immunity; accelerating wound healing; and serving as anti-inflammatory, antioxidant, antibacterial, and antiviral factors [6–12].

The modulatory and anti-inflammatory activity of *S. platensis* is executed under the regulation of several significant mediators, such as IL-2, IL-4, TNF-α, IL-1β, IL-6, IL-10, and COX-2, which have the ability to inhibit or stimulate the transcription factor NF-κB [9, 13, 14]. The anti-inflammatory mechanism of *S. platensis* is expressed through the inhibition of the nuclear translocation of NF-κB; this effect results in the subsequent inhibition of the expression of pro-inflammatory genes [15–19]. NF-κB is a transcription factor that plays an important role in various physiological and pathological processes. Two distinct NF-κB pathways that act through different activation mechanisms exist: canonical and noncanonical NF-κB pathways [20]. NF-κB is inactive in the cytoplasm because it is bound to inhibitory proteins, namely, IκB [21]. The canonical NF-κB pathway can be activated through the stimulation of multisubunit IκB kinase (IKK). Furthermore, the inhibitory protein IκBα (IκB subunit) bound to NF-κB is degraded after it is phosphorylated at a specific site. The IKK complex is activated by cytokines, mitogens, growth factors, stress agents, and microbial components [22]. The IKK complex consists of one subunit of the NF-κB essential modulator (NEMO) or IKKγ and two subunits (IKKA and IKKB) that have catalytic sites. The process mentioned above involves the rapid and temporary transfer of canonical NF-κB members, particularly the p50/RelA and p50/c-Rel dimers, from the cytoplasm to the nucleus [23]. Meanwhile, the noncanonical NF-κB pathway is activated by the degradation of NF-κB-inducing kinase (NIK) [24]. In addition, COX-2, the inflammatory mediator, was also reported negatively and positively regulate NF-κB [25].

In this study, we used molecular docking to determine the molecular interactions of the bioactive compounds of *S. platensis*, namely, phycocyanobilin [26], β-carotene [27], and α-glucan [28, 29], through the binding of the lead compounds to the proteins involved in the canonical and noncanonical activation pathways of NF-κB. This study aims to predict the potential of the bioactive compounds of *S. platensis* for modulating immune function by reducing inflammation through their ability to inhibit the NF-κB activation pathway.

## Methods

**In Silico molecular docking study.** The entire molecular docking process was performed by using an Asus device with an Intel(R) Core (TM) i3-1005G1 CPU @ 1.20 GHz 1.19 GHz with 4 GB RAM, Windows 10, and a 64-bit operating system. The software used to obtain and process the data were MarvinSketch-22.11.0, AutodockTools-1.5.6, Discovery Studio-V21.1.0.20298, swissADME, and Protox-II.

**Ligand preparation.** In this study, the bioactive compounds of *S. platensis* that were used as ligands were phycocyanobilin (PubChem IDs: 6438349) [26], β-carotene (PubChem IDs: 5280489) [27], and α-glucan (PubChem IDs: 134692111) [28, 29]. The biological interactions of these three bioactive compounds with the related indicators described in this study were predicted by using http://way2drug.com/passonline. In addition, the following inhibitors against target proteins were used as control ligands: parthenolide (PubChem IDs:7251185) [30], BAY-11-7082 ([E]-3-tosylacrylonitrile), PubChem IDs:5353431) [31], celecoxib (PubChem IDs:2662), and rofecoxib (PubChem IDs: 5090) [32]. First, the PubChem® database was used to derive the three-dimensional (3D) structure of the third ligand. Then, by using MarvinSketch-22.11.0, the entire ligand structure was optimized into three dimensions and converted into a .pdb file. Finally, by using AutoDockTools-1.5.6, all the ligands were charged, the torsion was set, and the result was saved in .pdbqt file format so that the ligands would be ready for use.

**Protein preparation.** The target proteins used in this study were the proteins involved in the NF-κB activation pathway, namely, NEMO–IKK, IKK1/IKKA, IKK2/IKKB, NIK, IκBα-NF-κB, NF-κB, and COX-2. The proteins NEMO (IKBKG), IKKA (CHUK), IKKB (IKBKB), NIK (MAP4K4), IκBα (NFKBIA), NFKBp65 (Nfkb3/RELA), NFKBp50 (Nfkb1/NFKB1), and COX-2 (PTGS2) were then analyzed by using protein–protein interaction software (https://string-db.org/) to determine if they were associated with each other. All protein structures were obtained from the Protein Data Bank (www.rscb.org) in .pdb file format. Each protein structure was then removed molecularly. Then, nonpolar hydrogens and Gasteiger charges were added, and the result was converted into .pdbqt file format. All stages of this preparation process were performed by using AutoDockTools-1.5.6 software. The grid box size and coordinate position of the grid center were adjusted by using blind docking for the following proteins: NEMO–IKK (PDB ID: 3BRT), the IκBα–NF-κB complex (PDB ID: 1IKN), and NF-κB p65/p50 (PDB ID: 1VKX). The grid box size used for the NEMO–IKK and IκBα-NF-κB complex proteins was 60 × 60 × 60 and that for the NF-κB protein around the active site was 60 × 120 × 60. Through validation with native protein ligands, the grid box sizes and grid center coordinate positions of IKK1/IKKA (PDB ID: 5EBZ), IKK2/IKKB (PDB ID:4KIK), NIK (PDB ID: 4IDV), and COX-2 (PDB ID:5KIR) were found to be 60 × 60 × 60 around the active site.

**Molecular docking.** Docking files were prepared in .gpf and .dpf formats by using the AutoDockTools-1.5.6 software before ligand and protein docking. The search parameter used was the Lamarckian genetic algorithm. Docking was done online by using the command-line interpreter Command Prompt. The docking results were analyzed in .dlg format by using AutoDockTools-1.5.6 software on the basis of the binding value (ΔG), the inhibition energy constant (Ki), and the amount of hydrogen binding. The docking results were visualized by using Discovery Studio Software [33, 34].

**Toxicity prediction In Silico.** The toxicity analysis, which was based on the prediction results of oral toxicity, classified toxicity as organ toxicity (hepatotoxicity) and the end point of toxicity, namely, mutagenicity, carcinogenicity, and cytotoxicity. In addition, drug-likeness parameters, gastrointestinal absorption, Lipinski rules, and the predicted interactions with significant cytochromes can be determined to avoid potential interactions with other medications. Each compound's canonical SMILES was obtained from PubChem and entered on the SwissADME and Protox-II platforms to obtain the toxicity predictions for the three active compounds and the inhibitors used.

## Results

The target proteins (Table 1 and Supplementary Table 1) used in the molecular docking portion of this study are proteins that are involved in the NF-κB activation pathway: NEMO–IKK, IKK1/IKKA, IKK2/IKKB, NIK, IκBα-NF-κB, NF-κB, and COX-2.[20,35,36] The protein–protein interaction network analysis (Figure 1) among NEMO (IKBKG), IKKA (CHUK), IKKB (IKBKB), NIK (MAP4K4), IκBα (NFKBIA), NFKBp65 (Nfkb3/RELA), and NFKBp50 (Nfkb1/NFKB1) revealed that the proteins, with the exception of COX-2 (PTGS2), have strong associations with each other as evidenced by their scores, which fell within 0.900–0.999 (highest confidence) (Supplementary Table 2) [37, 38]. The association score of COX-2 with the other proteins is between 0.569 and

0.795 (medium confidence–high confidence) [37, 38]. NF-κB, as the transcription factor of pro-inflammatory mediators, can be reasonably concluded to regulate the expression of COX-2 after regulation by the major pro-inflammatory cytokine TNF-α and IL-6. The indirect association between COX-2 and the other protein targets in this research can be explained by the positive feedback mechanism of COX-2 that increases NF-κB activity. Furthermore, the prostaglandin cyclopentanone has a negative feedback mechanism that inhibits NF-κB activity [25]. The three active compounds of *S. platensis* used in this work are phycocyanobilin, β-carotene, and α-glucan. The biological activity prediction anticipates that phycocyanobilin has biological activity as a protein kinase inhibitor; β-carotene acts as a TNF-expression inhibitor and anti-inflammatory; and α-glucan functions as an immunomodulator, an anti-inflammatory, an immunostimulant, and a nonsteroidal anti-inflammatory agent (Table 2) [39].

**Table 1. Summary of the Bioactive Compounds of *S. platensis* with the Best Affinity for Molecular Docking in the NF-κB Activation Pathway**

| No | Protein Target | Ligand | Active Compound | ΔG (kcal/mol) | pKi |
|---|---|---|---|---|---|
| 1 | NEMO–IKK | Control ligand (inhibitor) | Parthenolide | −7.03 | 7.09 µM |
| | | Test ligand | **β-Carotene** | −10.05 | 43.27 nM |
| 2 | IKK1/IKKA | Control ligand (inhibitor) | Parthenolide | −8.4 | 699.85 nM |
| | | Test ligand | **Phycocyanobilin** | −7.52 | 3.1 µM |
| 3 | IKK2/IKKB | Control ligand (inhibitor) | Parthenolide | −8.03 | 1.29 µM |
| | | Test ligand | **Phycocyanobilin** | −11.08 | 7.6 nM |
| 4 | NIK | Control ligand (inhibitor) | Parthenolide | −7.46 | 3.41 µM |
| | | Test ligand | **Phycocyanobilin** | −10.96 | 9.23 nM |
| 5 | IκBα-NF-κBp65/p50 | Control ligand (inhibitor) | BAY-11-7082 | −8.1 | 1.15 µM |
| | | Test ligand | **Phycocyanobilin** | −7.62 | 2.58 µM |
| 6 | NF-κBp65/p50 | Control ligand (inhibitor) | Parthenolide | −6.29 | 24.69 µM |
| | | Test ligand | **β-Carotene** | −8.64 | 463.53 nM |
| 7 | COX-2 | Control ligand (inhibitor) | Celecoxib | −11.01 | 8.51 nM |
| | | Control ligand (inhibitor) | Rofecoxib | −10.15 | 36.35 nM |
| | | Test ligand | **α-Glucan** | −6.93 | 8.29 µM |

ΔG (mean binding energy); pKi (binding affinity)

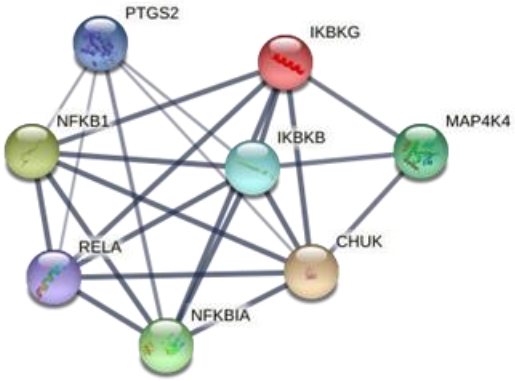


**Figure 1. Protein–protein Interaction Network Involving NEMO (IKBKG), IKKA (CHUK), IKKB (IKBKB), NIK (MAP4K4), IκBα (NFKBIA), NFKBp65 (Nfkb3/RELA), NFKBp50 (Nfkb1/NFKB1), and COX-2 (PTGS2). Interaction Score > 0.4 was Applied to Construct the Network [37, 38].**

**Table 2. Biological Activity Prediction for *S. platensis* Bioactive Compounds [39]**

| No | *S. platensis* bioactive compound | Pa | Pi | Activity |
|---|---|---|---|---|
| 1 | Phycocyanobilin | 0.457 | 0.045 | Kinase inhibitor |
| 2 | β-Carotene | 0.890 | 0.002 | TNF-expression inhibitor |
| | | 0.690 | 0.017 | Anti-inflammatory |
| 3 | α-Glucan | 0.557 | 0.007 | Immunomodulator |
| | | 0.729 | 0.012 | Anti-inflammatory |
| | | 0.873 | 0.005 | Immunostimulant |
| | | 0.464 | 0.015 | Nonsteroidal anti-inflammatory agent |

*Pa and Pi: Probabilities of the presence and absence of activity

The model of energetic ligand binding to the binding site on the target protein was predicted by using molecular docking [40]. The main parameters used in analyzing molecular docking results are the binding energy (ΔG) and the inhibition constant (Ki) [41]. The values of G and Ki determine the binding affinity for the receptor. A highly negative G value is indicative of the high binding affinity for the receptor's active site [41]. The best molecular docking result between the protein targets and bioactive compounds of *S. platensis* are presented in Table 1. Then, their 3D (Figure 2-8 (a-b)) and two-dimensional (2D, Figure 2-8 (c)) visualizations were generated by using Discovery Studio Software.

The interaction of the three *S. platensis* bioactive compounds with NEMO–IKK shows that β-carotene is the bioactive compound with the lowest G value of −10.05 kcal/mol (Table 1). Figure 2 illustrates that β-carotene binds to NEMO–IKK at the amino acid residues LYS90 and MET735. Moreover, β-carotene, together with other test ligands, binds to NEMO–IKK binding sites (Supplementary Table 1, Figure 2 (b-c)) that involve the amino acid residues ARG87, PHE82, GLU89, GLN86, LYS90, and GLN730 [30, 42].

In the molecular docking of the three bioactive compounds from *S. platensis* used against IKK1/IKKA, IKK2/IKKB, NIK, and the IκBα/NF-κB complex, phycocyanobilin shows potential as the compound with the lowest G values of −7.52, −11.08, −10.96, and −7.62 kcal/mol, respectively (Table 1). In the molecular docking of phycocyanobilin against IKK1/IKKA (Figure 3), the interaction occurs at the amino acid residues ARG20, THR23, and GLU89, which are amino acids that are also involved in the binding with the following test ligands: GLY22, CYS98, LEU21, VAL29, ILE164, VAL151, LYS44, ASN149, ARG20, and THR23 (Supplementary Table 1, Figure 3 (b-c)). The interactions of the amino acid residues CYS99, LYS106, LEU21, ASP103, GLY22, and GLN100 are shown in the visualization of the binding of the phycocyanobilin molecule to IKK2/IKKB (Figure 4). The same amino acid residues also interact with other test ligands with IKK2/IKKB, namely, CYS99, LEU21, GLY22, VAL74, ALA42, LYS106, LEU21, ASP103, VAL152, and VAL29 (Supplementary Table 1, Figure 4 (b-c)).

The visualization of the phycocyanobilin interaction with NIK (Figure 5) shows that the amino acid residues ARG408, SER410, ARG416, and ARG66 interact through a hydrogen bond. All test ligands at the binding site involve the same amino acids, i.e., ARG416, LEU472, ARG408, LEU522, VAL414 GLU473, A4RG-NF, ARG405, SER476, MET469, CYS533, and LEU522 (Supplementary Table 1, Figure 5 (b-c)) [43]. As shown in Figure 6, phycocyanobilin interacts with the IκBα–NF-κB complex by the binding to the amino acid residues LYS221, GLU286, PRO281, GLU222, and ALA242. Together with other test ligands, this interaction involves the same amino acids, specifically, HIS245, ARG246, LYS221, VAL244, GLU222, SER288, GLU284, and TYR251 (Supplementary Table 1, Figure 6 (b-c)).

The interactions of these three compounds with the NF-κB complex demonstrates that β-carotene is the bioactive compound with the lowest G value of −8.64 kcal/mol (Table 1). The visualization illustrates that the interaction of β-carotene with the NF-κB complex (Figure 7) involves the amino acid residues LEU154, ARG187, ALA188, LYS218, CYS120, ARG605, LYS575, VAL603, PHE34, TYR36, HIS88, and HIS604. The interactions of all the test ligands with the NF-κB complex involve the same amino acid residues: LYS195, ARG33, ARG605, LYS195, ASP217, ARG187, ARG605, VAL603, and PRO600 (Supplementary Table 1, Figure 7 (b-c)) [30]. Molecular docking was also performed with COX-2. However, the binding energies of the bioactive compounds of *S. platensis* are lower than those of COX-2 inhibitors, such as rofecoxib and celecoxib, with α-glucan (−6.93 kcal/mol) resulting in the lowest value among the bioactive compounds of *S. platensis*. The visualization of the protein ligand complex

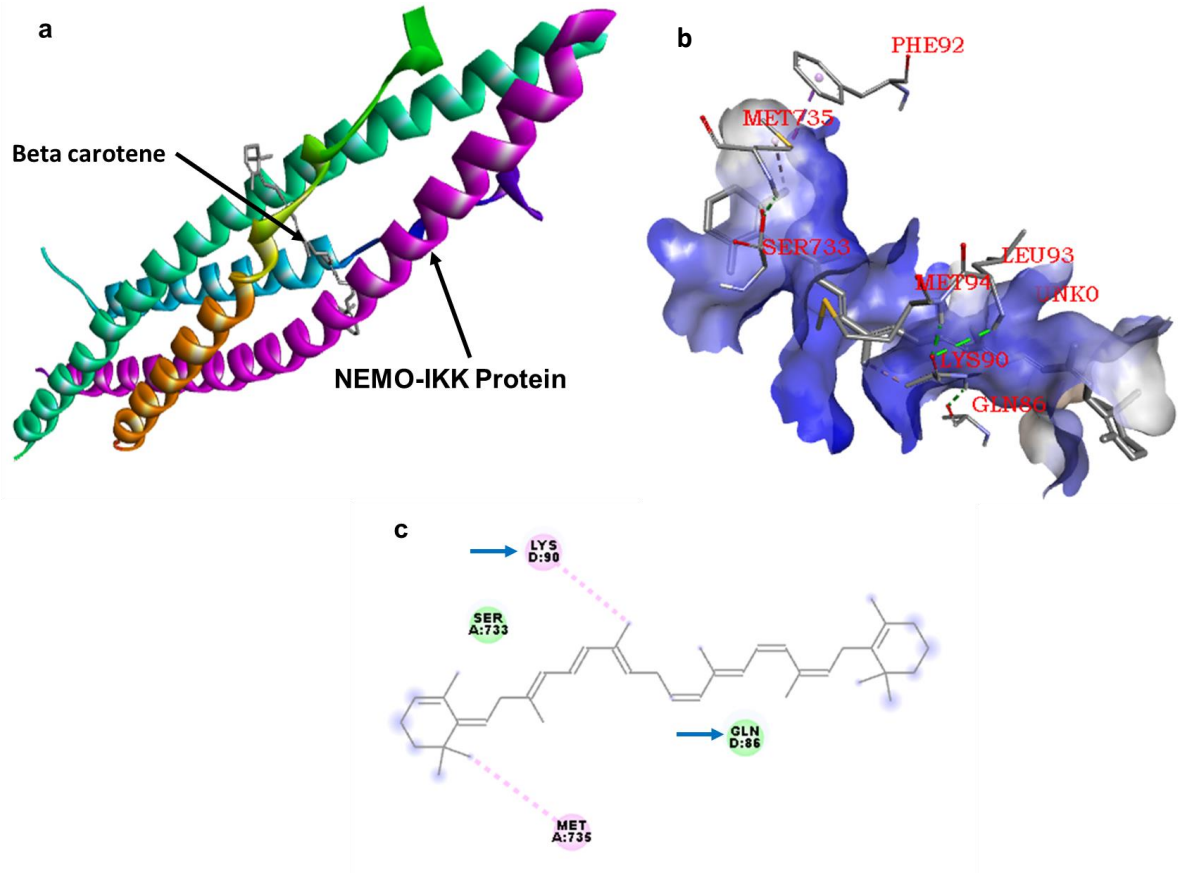


**Figure 2. 3D (a and b) and 2D (c: Arrow Represents the Same Amino Acid Residue that Binds to Other Ligands) Visualization of the Molecular Docking of the Bioactive Compounds of *S. platensis* with the Best Affinity for the NEMO/IKK Protein: Complex of β-carotene with the NEMO/IKK Protein**

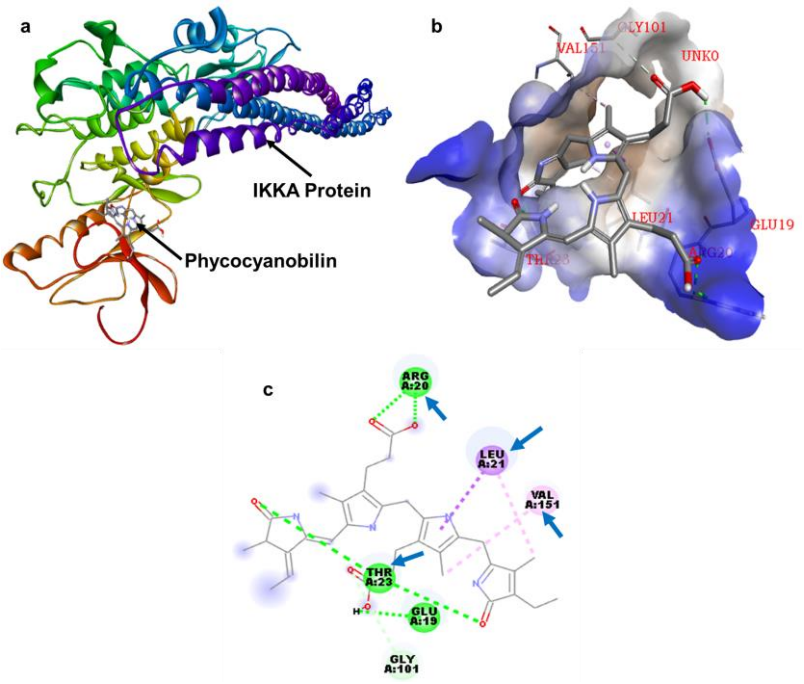


**Figure 3. 3D (a and b) and 2D (c: Arrow Represents the Same Amino Acid Residue that Binds to Other Ligands) Visualization of the Molecular Docking of the Bioactive Compounds of *S. platensis* with the Best Affinity for the IKK1/IKKA Protein: Complex of Phycocyanobilin with the IKK1/IKKA Protein**

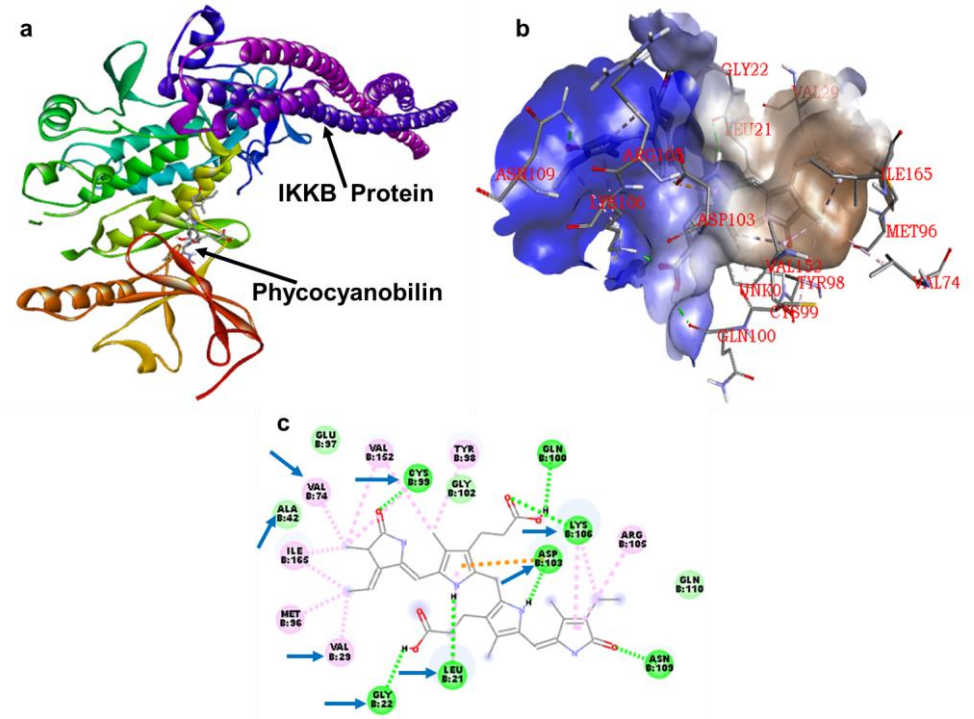


**Figure 4. 3D (a and b) and 2D (c: Arrow Represents the Same Amino Acid Residue that Binds to Other Ligands) Visualization of the Molecular Docking of the Bioactive Compound of *S. platensis* with the Best Affinity for the IKK2/IKKB Protein: Complex of Phycocyanobilin with the IKK2/IKKB Protein**

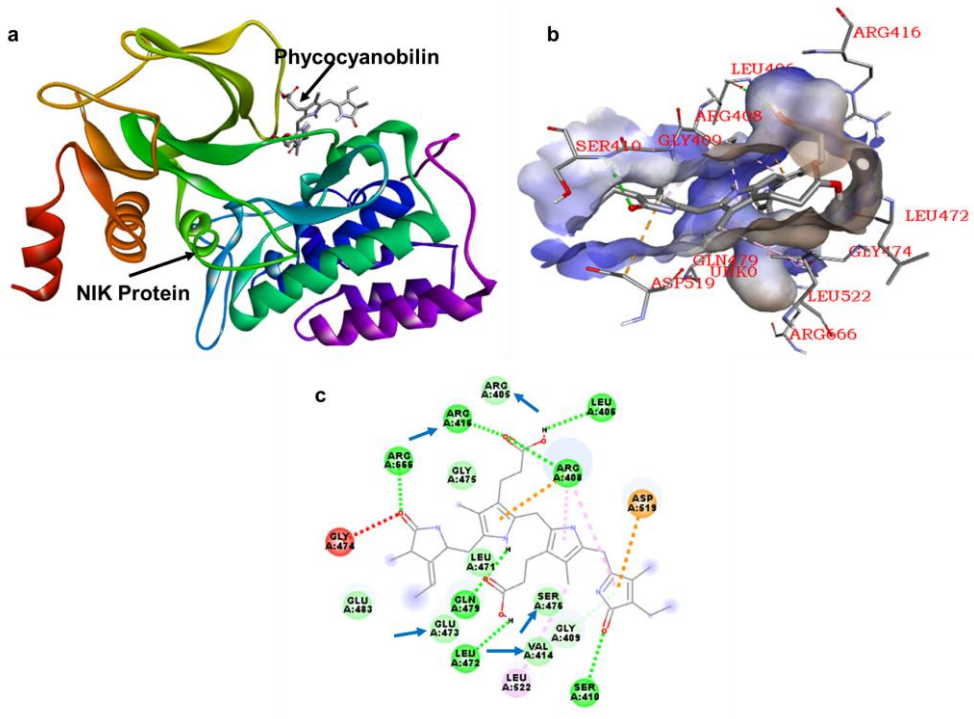


**Figure 5. 3D (a and b) and 2D (c: Arrow Represents the Same Amino Acid Residue that Binds to Other Ligands) Visualization of the Molecular Docking of the Bioactive Compound of *S. platensis* with the Best Affinity for the NIK Protein: Complex of Phycocyanobilin with the NIK Protein**

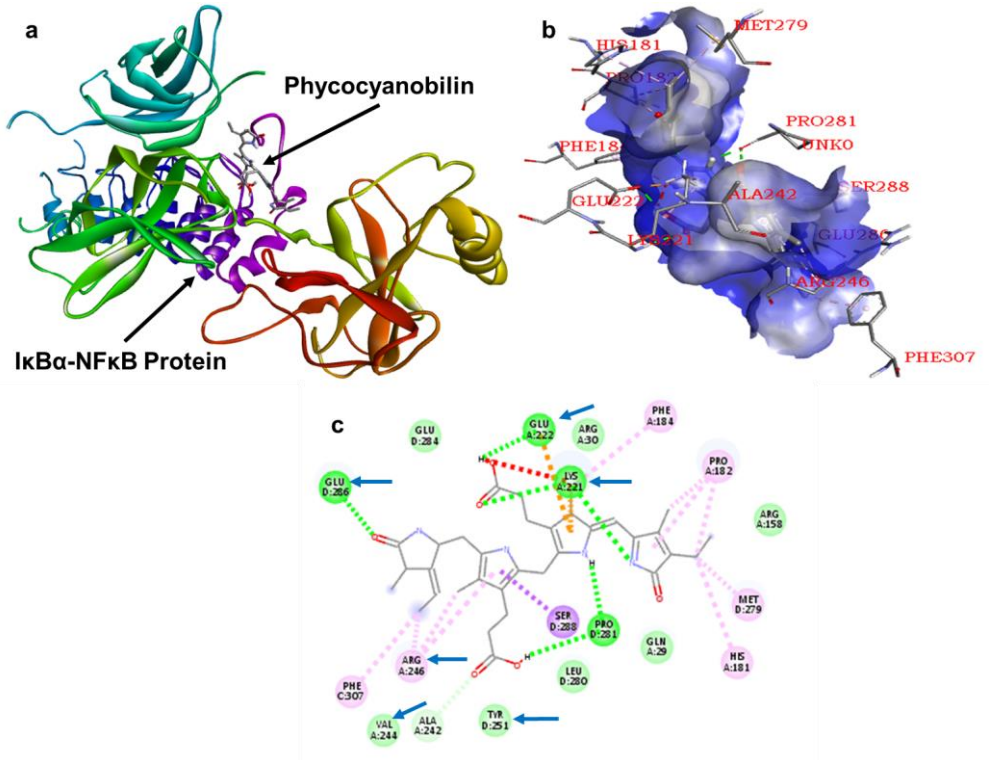


**Figure 6. 3D (a and b) and 2D (c: Arrow Represents the Same Amino Acid Residue that Binds to Other Ligands) Visualization of the Molecular Docking of the Bioactive Compound of *S. platensis* with the Best Affinity for the IkBα–NF-κB Complex Protein: Complex of Phycocyanobilin Binding with the IkBα–NF-κB Protein Complex**

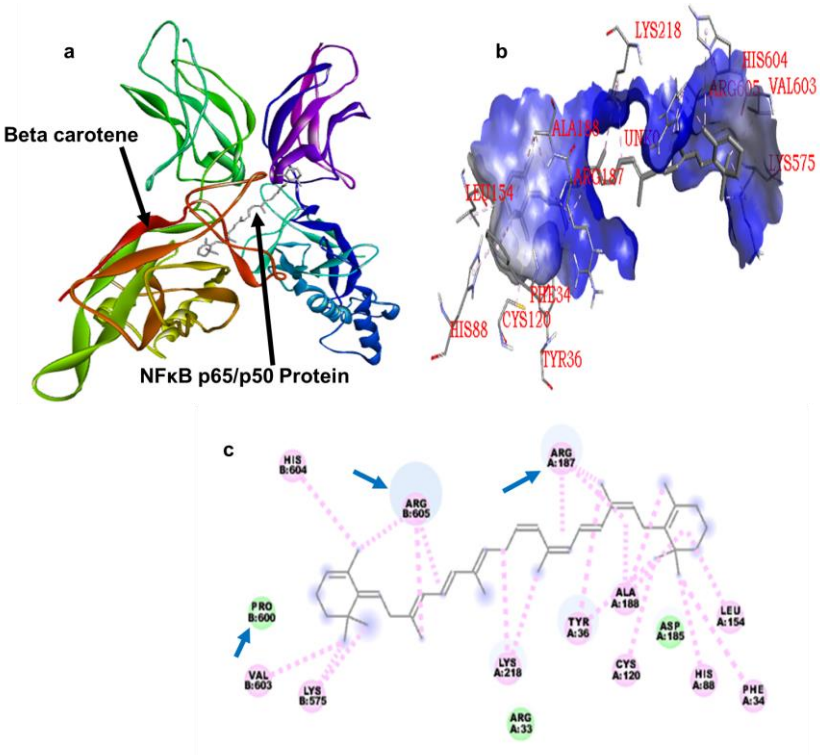


**Figure 7. 3D (a and b) and 2D (c: Arrow Represents the Same Amino Acid Residue that Binds to Other Ligands) Visualization of the Molecular Docking of the Bioactive Compound of *S. platensis* with the Best Affinity for the NF-κB Protein Complex: Complex of β-carotene with the NF-κB Protein Complex**

comprising COX-2 and α-glucan (Figure 8) shows that the involvement of the amino acids ARG513, PHE518, TYR355, SER530, MET522, SER530, and GLN192 occurs through hydrogen bonding with α-glucan. The test ligands used in this study interact with several of the same amino acids (Supplementary Table 1, Figure 8 (b-c)), i.e., ARG513, PHE518, LEU352, SER353, HIS90, TYR355, SER530, LEU531, and MET522 [32].

The results of the toxicity prediction (Table 3) with the Protox-II platform indicate that all the bioactive compounds of *S. platensis*, except for β-carotene, which has the mutagenicity risk of 0.71, lack toxicity risk. Meanwhile, parthenolide is predicted to pose carcinogenic risk with the probability of 0.52 and has the probability of 0.98 to impart the same adverse effects as xenobiotics on the immune system. In addition, celecoxib poses a carcinogenic risk with a probability of 0.56. Phycocyanobilin, β-carotene, and α-glucan (Table 4) also lack any potential interactions with the cytochromes CYP1A2, CYP2C19, CYP2C9, CYP2D6, and CYP3A4. All of the active ingredients of *S. platensis* are also predicted to be absorbed by the gastrointestinal tract even at low levels (Table 4) [44].

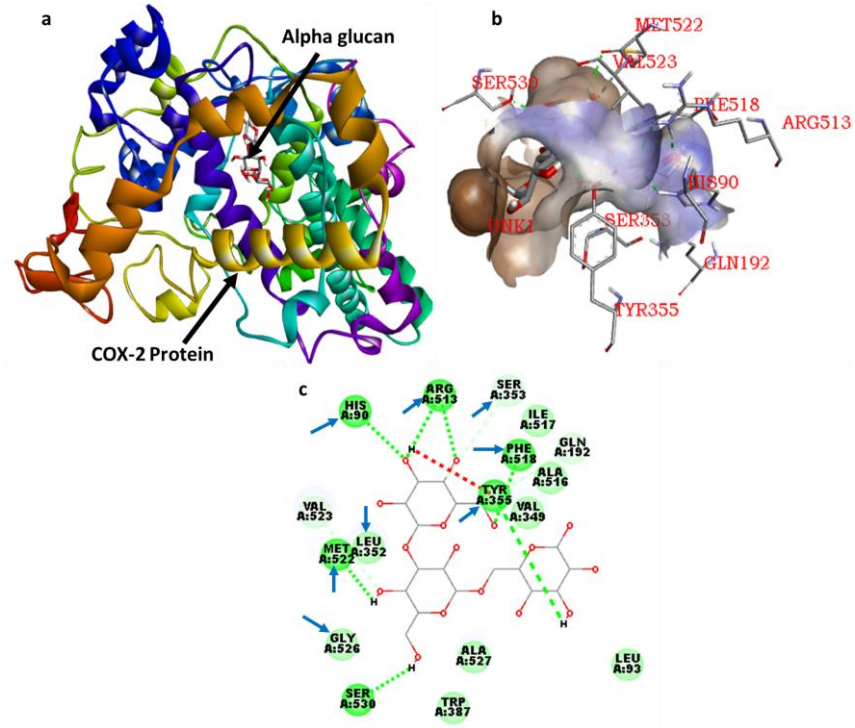


**Figure 8. 3D (a and b) and 2D (c: Arrow Represents the Same Amino Acid Residue that Binds to Other Ligands) Visualization of the Molecular Docking of the Bioactive Compound of *S. platensis* with the Best Affinity for the COX-2 Protein: Complex of α-glucan with the COX-2 Protein**

**Table 3. Toxicity Prediction of the Bioactive Compounds and Inhibitors of *S. platensis***

| Classification | Target | Parthenolide | | BAY-11-7082 | | Celecoxib | | Rofecoxib | | Phycoyanobilin | | β-carotene | | α-glucan | |
|---|---|---|---|---|---|---|---|---|---|---|---|---|---|---|---|
| | | **1** | **2** | **1** | **2** | **1** | **2** | **1** | **2** | **1** | **2** | **1** | **2** | **1** | **2** |
| Oral toxicity prediction | Predicted LD50 | 1330 mg/kg | | 1440 mg/kg | | 1400 mg/kg | | 2240 mg/kg | | 3066 mg/kg | | 1510 mg/kg | | na | |
| | Predicted Toxicity Class | 4 | | 4 | | 4 | | 5 | | 5 | | 4 | | n.a | |
| Organ Toxicity | Hepatotoxicity | IA | 0.77 | IA | 0.85 | IA | 0.98 | IA | 0.55 | IA | 0.73 | IA | 0.85 | IA | 0.9 |
| Toxicity end points | Carcinogenicity | A | 0.52 | IA | 0.73 | A | 0.56 | IA | 0.71 | IA | 0.6 | IA | 0.86 | IA | 0.9 |
| | Immunotoxicity | A | 0.98 | IA | 0.99 | IA | 0.99 | IA | 0.97 | IA | 0.96 | IA | 0.88 | IA | 1 |
| | Mutagenicity | IA | 0.74 | IA | 0.81 | IA | 0.82 | IA | 0.68 | IA | 0.7 | A | 0.71 | IA | 0.9 |
| | Cytotoxicity | IA | 0.81 | IA | 0.79 | IA | 0.79 | IA | 0.76 | IA | 0.6 | IA | 0.81 | IA | 0.8 |

**1** (Prediction); **2** (Probability); IA (Inactive); A (Active)

**Table 4. ADME Parameter Prediction of the Three Active Compounds of *S. platensis* and Inhibitors**

| Pharmacological Parameter | Parthenolide | (E)-3-Tosylacry-lonitrile | Celecoxib | Rofecoxib | Phycocyanobilin | β-Carotene | α-Glucan |
|---|---|---|---|---|---|---|---|
| MW (g/mol) | 248.32 g/mol | 207.25 g/mol | 381.37 g/mol | 314.36 g/mol | 586.68 g/mol | 536.87 g/mol | 504.44 g/mol |
| HBA | 3 | 3 | 7 | 4 | 7 | 0 | 16 |
| HBD | 0 | 0 | 1 | 0 | 5 | 0 | 11 |
| LogP | 2.64 | 1.79 | 3.4 | 2.79 | 3.74 | 11.11 | −5.32 |
| GI Abs | High | High | High | High | Low | Low | Low |
| Lipinski | Yes | Yes | Yes | Yes | Yes | Yes | No |
| CYPIA2 inhibitor | No | Yes | Yes | Yes | No | No | No |
| CYP2C19 inhibitor | No | No | No | Yes | No | No | No |
| CYP2C9 inhibitor | No | No | Yes | Yes | No | No | No |
| CYP2D6 inhibitor | No | No | No | No | No | No | No |
| CYP3A4 inhibitor | No | No | No | No | No | No | No |

## Discussion

In addition to drug discovery, computational techniques can be used in functional food research to identify complementary ingredients and targets through predictive molecular modeling. Several studies on the development of functional foods have utilized bioinformatics applications to predict toxicity [45]. Moreover, some works have predicted the molecular interactions of the bioactive compounds of *S. platensis* as anti-inflammatory components [43, 44]. However, these interaction studies did not review the complex modulation of the NF-κB activation pathway.

In this study, docking was conducted to analyze the predicted molecular interactions of several bioactive compounds of *S. platensis* that have been identified to have potential interactions with the NF-κB activation pathway, specifically with NEMO–IKK, IKK1/IKKA, IKK2/IKKB, NIK, IκBα-NF-κB, NF-κB, and COX-2 [20, 25, 35, 36]. These proteins were chosen because of their involvement in direct and indirect inflammatory reactions. Many therapeutic strategies for inflammatory diseases aim to block NF-κB activity because NF-κB signaling plays a vital role in these diseases [46].

Through the inhibition of IKK kinase activity, some drugs, such as aspirin and salicylates, prevent IκBα phosphorylation. Other drugs, including lactacystin and PS-34, block IκBα degradation by inhibiting protease activity. Tacrolimus has been reported to be an IκBα repressor that prevents the NF-κB subunits of RelA, p50, c-Rel, and other members from entering the nucleus. Other drugs, for example, glucocorticoids and PPAR agonists, can prevent the NF-κB subunit from binding to the target gene and further inhibit transcription [14].

The FDA states that functional foods are part of a normal diet and consist of nutrients consumed in a food matrix that can improve health and exert physiological effects through one or more active ingredients [45]. *S. platensis*, whose nutritional content can potentially improve human health through various means, can be used as a functional food ingredient [47]. *S. platensis* is rich in various bioactive compounds, including phycocyanin, polyunsaturated fatty acids, polysaccharides, γ-linolenic acid, phenolic compounds, carotenoids, minerals, vitamins, and several minerals that are important for bodily nutrition [48]. Various studies have been conducted to determine the effectiveness of each active ingredient, including phycocyanobilin, β-carotene (a carotenoid), and α-glucan (a polysaccharide), which have potential applications as anti-inflammatories, immunomodulatories, and antioxidants [28, 49, 50].

In the molecular docking carried out in this study, parthenolide [30] was used as the control ligand inhibitor of the NF-κB activation pathway through interactions with the proteins NEMO–IKK, IKK1/IKKA, IKK2/IKKB, NIK, IκBα/NF-κB, and NF-κB. Through molecular docking, phycocyanobilin was demonstrated to potentially inhibit the NF-κB activation pathway via its interaction with the IKK1/IKKA, IKK2/IKKB, NIK, and NF-κB proteins. β-Carotene also showed its potential as an inhibitor in binding assays with NEMO–IKK and the NF-κB complex [43].

The molecular docking results in this study indicated the potential of the active ingredients of *S. platensis* as inhibitors acting through the IκBα–NF-κB complex. Although the binding energy of phycocyanobilin (–7.62) was not lower that of BAY 11-7082 (−8.1 kcal/mol), phycocyanobilin had the lowest binding energy when compared with β-carotene and α-glucan. In addition, the binding sites of phycocyanobilin and the other two active ingredients are in the region that involves the same amino acids as the inhibitor BAY 11-7082 [31]. This study demonstrated that the binding energy of COX-2

by α-glucan (−6.93 kcal/mol) was lower than that by phycocyanobilin (−5.38 kcal/mol) and β-carotene (−5.98 kcal/mol). However, this binding energy was suboptimal compared with the binding energy of the control ligands, namely, celecoxib (−11.01 kcal/mol) and rofecoxib (−10.15 kcal/mol).

The molecular docking results for the three active ingredients of *S. platensis* used in this study further emphasize their anti-inflammatory potential. The molecular docking in this study yielded results regarding the potency of α-glucan that were different from those provided by in vitro tests. α-Glucan from *S. platensis* was found to significantly increase IL-6 mRNA expression and may thus have immunomodulatory activity [50]. Another study by Grzanna *et al*. 2006 [51] reported that supplementation with *S. platensis* polysaccharide increased NF-κB activation, which further increased the expression of the pro-inflammatory cytokines TNF-α and IL-1β, as well as the inflammatory mediator COX-2 [51].

Phycocyanobilin, β-carotene, and α-glucan were predicted to not exhibit any interactions with cytochromes that are representative of CYP450s in humans. Therefore, this prediction indicates that these bioactive compounds are likely safe for consumption even by patients undergoing other treatments [44].

## Conclusions

The potential as anti-inflammatories of the bioactive compounds of *S. platensis*, namely, phycocyanobilin, β-carotene, and α-glucan, can be predicted through molecular docking studies with various proteins involved in the NF-κB activation pathway. Phycocyanobilin shows good potential as an inhibitor in molecular docking with IKK1/IKKA, IKK2/IKKB, NIK, and the IκBα/NF-κB complex. Furthermore, β-carotene has good potential as an inhibitor through its interaction with NEMO–IKK and the NF-κB complex, and α-glucan has potential as an inhibitor through interactions with COX-2. Therefore, supplementation with a complete set of these bioactive compounds is expected to provide optimal benefits. However, further in vitro and in vivo research is essential to evaluate the function of *S. platensis* as a functional food.

## Acknowledgments

The authors thank Aisyah Fitriannisa Prawiningrum for technical assistance and useful discussion.

## Supplementary Data

Supplementary Table 1. Comparison of ΔG values, Ki, and amino acid residues involved in the interaction of the bioactive compounds of *S. platensis* and the control inhibitors of the NF-κB activation pathway

Supplementary Table 2. Protein–Protein Interaction: NEMO (IKBKG), IKK1/IKKA (CHUK), IKK2/IKKB (IKBKB), NIK (MAP4K4), IκBα-NFκB Complex (NFKBIA), NF-κB p65 (RELA), NF-κB p50 (NFKB1), COX-2 (PTGS2)

## References

[1] Borgoni, S., Kudryashova, K.S., Burka, K., de Magalhães, J.P. 2021. Targeting immune dysfunction in aging. Ageing Res. Rev. 70: 101410, https://doi.org/10.1016/j.arr.2021.101410.

[2] Lyons, C.L., Kennedy, E.B., Roche, H.M. 2016. Metabolic inflammation-differential modulation by dietary constituents. Nutrients. 8(5): 247, https://doi.org/10.3390/nu8050247.

[3] Grover, P., Bhatnagar, A., Kumari, N., Bhatt, N.A., Nishad, K.D., Purkayastha, J. 2021. C-Phycocyanin-a novel protein from Spirulina platensis- In vivo toxicity, antioxidant and immunomodulatory studies. Saudi J. Biol. Sci. 28(3): 1853–1859, https://doi.org/10.1016/j.sjbs.2020.12.037.

[4] Sorrenti, V., Castagna, D.A., Fortinguerra, S., Buriani, A., Scapagnini, G., Willcox, D.C. 2021. Spirulina microalgae and brain health: A scoping review of experimental and clinical evidence. Mar. Drugs. 19(6): 1–12, https://doi.org/10.3390/md19060293.

[5] Khan, Z., Bhadouria, P., Bisen, P. 2005. Nutritional and Therapeutic Potential of Spirulina. Curr. Pharm. Biotechnol. 6(5): 373–379, https://doi.org/10.2174/138920105774370607.

[6] Wu, Q., Liu, L., Miron, A., Klímová, B., Wan, D., Kuča, K. 2016. The antioxidant, immunomodulatory, and anti-inflammatory activities of Spirulina: an overview. Arch. Toxicol. 90(8): 1817–1840, https://doi.org/10.1007/s00204-016-1744-5.

[7] Wang, Z., Wang, Y., Zhang, Z., Wang, X. 2016. Purification and identification of antioxidant peptides from wheat gluten hydrolysates. J. Chin. Cereal Oils Assoc. 31(5): 17–21.

[8] Ali, H.E.A., Shanab, S.M.M., Abo-State, M.A.M., Shalaby, E.A.A., El Demerdash, U.M.N., Abdullah, MA. 2014. Evaluation of antioxidants, pigments and secondary metabolites contents in Spirulina platensis. Appl. Mech. Mater. 625: 160–163, https://doi.org/10.4028/www.scientific.net/AMM.625.160.

[9] Balachandran, P., Pugh, N.D., Ma, G., Pasco, D.S. 2006. Toll-like receptor 2-dependent activation of monocytes by Spirulina polysaccharide and its immune enhancing action in mice. Int. Immunopharmacol. 6(12): 1808–1814, https://doi.org/10.1016/j.intimp.2006.08.001.

[10] Seyidoglu, N., Köseli, E., Gurbanli, R., Aydin, C. 2021. The preventive role of Spirulina platensis (*Arthrospira platensis*) in immune and oxidative insults in a stress-induced rat model. J. Vet. Res.

65(2): 193–200, https://doi.org/10.2478/jvetres-2021-0033.
[11] Soltani, M., Khosravi, A.R., Asadi, F., Shokri, H. 2021. Evaluation of protective efficacy of Spirulina platensis in Balb/C mice with candidiasis. J. Mycol. Med. 22(4): 329–334, https://doi.org/10.1016/j.mycmed.2012.10.001.
[12] Elbialy, Z.I., Assar, D.H., Abdelnaby, A., Asa, S.A., Abdelhiee, E.Y., Ibrahim, S.S., *et al*. 2021. Healing potential of Spirulina platensis for skin wounds by modulating bFGF, VEGF, TGF-ß1 and α-SMA genes expression targeting angiogenesis and scar tissue formation in the rat model. Biomed. Pharmacother. 137: 111349, https://doi.org/10.1016/j.biopha.2021.111349.
[13] Mao, T.K., Gershwin, M.E. 2005. Effects of a Spirulina-Based Dietary Supplement on Cytokine Production from Allergic Rhinitis Patients. J. Med. Food. 8(1): 27–30.
[14] Liu, T., Zhang, L., Joo, D., Sun, S.C. 2017. NF-κB signaling in inflammation. Signal Transduct Target. Ther. 2(1): 17023, https://doi.org/10.1038/sigtrans.2017.23.
[15] Ku, C.S., Pham, T.X., Park, Y., Kim, B., Shin, M.S., Kang, I., *et al*. 2013. Edible blue-green algae reduce the production of pro-inflammatory cytokines by inhibiting NF-κB pathway in macrophages and splenocytes. Biochim. Biophys. Acta-Gen. Subj. 1830(4): 2981–2988, https://doi.org/10.1016/j.bbagen.2013.01.018.
[16] Hwang, J.H., Chen, J.C., Chan, Y.C. 2013. Effects of C-phycocyanin and Spirulina on Salicylate-Induced Tinnitus, Expression of NMDA Receptor and Inflammatory Genes. Lewin A, editor. PLoS One. 8(3): e58215, https://doi.org/10.1371/journal.pone.0 058215.
[17] Al-Qahtani, W.H., Binobead, M.A. 2019. Anti-inflammatory, antioxidant and antihepatotoxic effects of Spirulina platensis against D-galactosamine induced hepatotoxicity in rats. Saudi J. Biol. Sci. 26(4): 647–652, https://doi.org/10.1016/j.sjbs.2018.01.003.
[18] Chen, J.C., Liu, K.S., Yang, T.J., Hwang, J.H., Chan, Y.C., Lee I.T. 2012. Spirulina and C-phycocyanin reduce cytotoxicity and inflammation-related genes expression of microglial cells. Nutr. Neurosci. 15(6): 252–256, https://doi.org/10.1179/1476830512Y.0000000020.
[19] Lee, J., Park, A., Kim, M.J., Lim, H.J., Rha, Y.A., Kang, H.G. 2017. Spirulina extract enhanced a protective effect in type 1 diabetes by anti-apoptosis and anti-ROS production. Nutrients. 9(12): 1–20, https://doi.org/10.3390/nu9121363.
[20] Liu, T., Zhang, L., Joo, D., Sun, S.C. 2017. NF-κB signaling in inflammation. Signal Transduct. Target. Ther. 2(1): 17023, https://doi.org/10.1038/sigtrans.2017.23.
[21] Karin, M., Ben-neriah, Y. 2000. Phosporilation meets the ubiquitination: The Control of NF- kapp B Activity. Annu. Rev. Immunol. 18: 621–663.
[22] Christian, F., Smith, E.L., Carmody, R.J. 2016. The regulation of NF-κB Subunits by Phosphorylation. Cells. 5(1): 12, https://doi.org/10.3390/cells5010012.
[23] Liu, T., Zhang, L., Joo, D., Sun, S.C. 2017. NF-κB signaling in inflammation. Signal Transduct. Target. Ther. 2(1): 17023, https://doi.org/10.1038/sigtrans.2017.23.
[24] Hayden, M.S., Ghosh, S. 2004. Signaling to NF-κB. Genes Dev. 18(18): 2195–2224, https://doi.org/10.1101/gad.1228704.
[25] Poligone, B., Baldwin, A.S. 2001. Positive and negative regulation of NF-κB by COX-2. Roles of different prostaglandins. J. Biol. Chem. 276(42): 38658–38664, https://doi.org/10.1074/jbc.M106599200.
[26] Shih, C.M., Cheng, S.N., Wong, C.S., Kuo, Y.L., Chou, T.C. 2009. Antiinflammatory and antihyperalgesic activity of C-phycocyanin. Anesth. Analg. 108(4): 1303–1310, https://doi.org/10.1213/ane.0b013e318193e919.
[27] Bai, S.K., Lee, S.J., Na, H.J., Ha, K.S., Han, J.A., Lee, H., *et al*. 2005. β-Carotene inhibits inflammatory gene expression in lipopolysaccharide-stimulated macrophages by suppressing redox-based NF-κB activation. Exp. Mol. Med. 37(4): 323–334, https://doi.org/10.1038/emm.2005.42.
[28] Wu, X., Liu, Z., Liu, Y., Yang, Y., Shi, F., Cheong, K.L., *et al*. 2020. Immunostimulatory Effects of Polysaccharides from Spirulina platensis In Vivo and Vitro and Their Activation Mechanism on RAW246.7 Macrophages. Mar. Drugs. 18(11): 538, https://doi.org/10.3390/md18110538.
[29] Li, J., Zhang, Y., Yang, S., Lu, Z., Li, G., Liu, J., *et al*. 2021. Isolation, Purification, Characterization, and Immunomodulatory Activity Analysis of α-Glucans from Spirulina platensis. ACS Omega. 6(33): 21384–21394, https://doi.org/10.1021/acsomega.1c02175.
[30] Dawood, M., Ooko, E., Efferth, T. 2019. Collateral Sensitivity of Parthenolide via NF-κB and HIF-α Inhibition and Epigenetic Changes in Drug-Resistant Cancer Cell Lines. Front. Pharmacol. 10: 542, https://doi.org/10.3389/fphar.2019.00542.
[31] Cai, S.Q., Zhang, Q., Zhao, X.H., Shi, J. 2021. The In Vitro Anti-Inflammatory Activities of Galangin and Quercetin towards the LPS-Injured Rat Intestinal Epithelial (IEC-6) Cells as Affected by Heat Treatment. Molecules. 26(24): 7495, https://doi.org/10.3390/molecules26247495.
[32] Taidi, L., Maurady, A., Britel, M.R. 2022. Molecular docking study and molecular dynamic simulation of human cyclooxygenase-2 (COX-2) with selected eutypoids. J. Biomol. Struct. Dyn. 40(3): 1189–

1204, https://doi.org/10.1080/07391102.2020.1823884.

[33] Pannindriya, P., Safithri, M., Tarman, K. 2021. Analisis In Silico Senyawa Aktif Sprirulina platensis sebagai Inhibitor Tirosinase. Jurnal Pengolah Hasil Perikanan Indonesia. 24(1): 70–77, https://doi.org/10.17844/jphpi.v24i1.33122.

[34] Saini, M.K., Sanyal, S.N. 2015. Cell cycle regulation and apoptotic cell death in experimental colon carcinogenesis: Intervening with cyclooxygenase-2 inhibitors. Nutr. Cancer. 67(4): 620–636, https://doi.org/10.1080/01635581.2015.1015743.

[35] Huxford, T., Ghosh, G. 2009. A Structural Guide to Proteins of the NF- B Signaling Module. Cold Spring Harb. Perspect. Biol. 1(3): a000075–a000075, https://doi.org/10.1101/cshperspect.a000075.

[36] Kracht, M., Müller-Ladner, U., Schmitz, M.L. 2020. Mutual regulation of metabolic processes and proinflammatory NF-κB signaling. J. Allerg. Clin. Immunol. 146(4): 694–705, https://doi.org/10.1016/j.jaci.2020.07.027.

[37] Szklarczyk, D., Gable, A.L., Lyon, D., Junge, A., Wyder, S., Huerta-Cepas, J., *et al*. 2019. STRING v11: Protein-protein association networks with increased coverage, supporting functional discovery in genome-wide experimental datasets. Nucleic Acids Res. 47(D1): D607–D613, https://doi.org/10.1093/nar/gky1131.

[38] Karimizadeh, E., Sharifi-Zarchi, A., Nikaein, H., Salehi, S., Salamatian B., Elmi N., *et al*. 2019. Analysis of gene expression profiles and protein-protein interaction networks in multiple tissues of systemic sclerosis. BMC Med. Genomics. 12(1): 199, https://doi.org/10.1186/s12920-019-0632-2.

[39] Druzhilovskiy, D.S., Rudik, A.V., Filimonov, D.A., Gloriozova, T.A., Lagunin, A.A., Dmitriev A.V., *et al*. 2017. Computational platform Way2Drug: from the prediction of biological activity to drug repurposing. Russ. Chem. Bull. 66(10): 1832–1841, https://doi.org/10.1007/s11172-017-1954-x.

[40] Ece, A. 2018. E-Pharmacophore Mapping Combined with Virtual Screening and Molecular Docking to Identify Potent and Selective Inhibitors of P90 Ribosomal S6 Kinase (RSK). Turkish J. Pharm. Sci. 13(2): 241–248, https://doi.org/10.4274/tjps.28290.

[41] Forli, S., Huey, R., Pique, M.E., Sanner, M.F., Goodsell, D.S., Olson, A.J. 2016. Computational protein–ligand docking and virtual drug screening with the AutoDock suite. Nat. Protoc. 11(5): 905–919, https://doi.org/10.1038/nprot.2016.051.

[42] Seo, E.J., Sugimoto, Y., Greten, H.J., Efferth, T. 2018. Repurposing of bromocriptine for cancer therapy. Front. Pharmacol. 9: 1030, https://doi.org/10.3389/fphar.2018.01030.

[43] Widyaningrum, D., Oktafika, R.A., Cecilia, D. 2022. Microalgae pigments as a promising immunomodulating food ingredient: In silico study. IOP Conf. Ser. Earth Environ. Sci. 998(1): 012056, https://doi.org/10.1088/1755-1315/998/1/012056.

[44] Petit, L., Vernès, L., Cadoret, J.P. 2021. Docking and in silico toxicity assessment of Arthrospira compounds as potential antiviral agents against SARS-CoV-2. J. Appl. Phycol. 33(3): 1579–1602, https://doi.org/10.1007/s10811-021-02372-9.

[45] Carpio, L.E., Sanz, Y., Gozalbes, R., Barigye, S.J. 2021. Computational strategies for the discovery of biological functions of health foods, nutraceuticals and cosmeceuticals: a review. Mol. Divers. 25(3): 1425–1438, https://doi.org/10.1007/s11030-021-10277-5.

[46] Sukumaran, G., Ezhilarasan, D., Ramani, P., Merlin, R.J. 2022. Molecular docking analysis of syringic acid with proteins in inflammatory cascade. Biomed. Inform. 18(3): 219–225, https://doi.org/10.6026/97320630018219.

[47] Finamore, A., Palmery, M., Bensehaila, S., Peluso, I. 2017. Antioxidant, Immunomodulating, and Microbial-Modulating Activities of the Sustainable and Ecofriendly Spirulina. Oxid Med. Cell. Longev. 2017(1): 1–14, https://doi.org/10.1155/2017/3247528.

[48] Han, P., Li, J., Zhong, H., Xie, J., Zhang, P., Lu, Q., *et al*. 2021. Anti-oxidation properties and therapeutic potentials of spirulina. Algal Res. 55: 102240, https://doi.org/10.1016/j.algal.2021.102240.

[49] Liu, Q., Huang, Y., Zhang, R., Cai, T., Cai, Y. 2016. Medical Application of Spirulina platensis Derived C-Phycocyanin. Evid.-Based Complement. Altern. Med. 2016: 1–14, https://doi.org/10.1155/2016/7803846.

[50] Li, J., Zhang, Y., Yang, S., Lu, Z., Li, G., Liu, J., *et al*. 2021. Isolation, Purification, Characterization, and Immunomodulatory Activity Analysis of α-Glucans from Spirulina platensis. ACS Omega. 6(33): 21384–21394, https://doi.org/10.1021/acsomega.1c02175.

[51] Grzanna, R., Polotsky, A., Phan, P.V., Pugh, N., Pasco, D., Frondoza, C.G. 2006. Immolina, a high-molecular-weight polysaccharide fraction of spirulina, enhances chemokine expression in human monocytic THP-1 cells. J. Altern. Complement. Med. 12(5): 429–435, https://doi.org/10.1089/acm.2006.12.429.

## Supplementary Data

**Supplementary Table 1. Comparison of ΔG values, Ki, and amino acid residues involved in the interaction of the bioactive compounds of *S. platensis* and the control inhibitors of the NF-κB activation pathway**

| No | Protein | Ligand | Active Compound | ΔG (kcal/mol) | pKi | Binding Residues |
|---|---|---|---|---|---|---|
| 1 | NEMO–IKK (PDB ID: 3BRT) | Control ligand (inhibitor) | Parthenolide (PubChem IDs: 7251185) | −7.03 | 7.09 µM | **GLN83*,** ARG87, PHE82, GLN730, THR726 |
| | | Test ligand (*S. platensis* bioactive compound) | Phycocyanobilin (PubChem IDs: 6438349) | −7.98 | 1.41 µM | **GLU89*, GLN86, ASN732*,** LYS90, GLU729, PHE82, SER85, MET734, LEU93, MET94, ASP725, GLN730 |
| | | | **β-Carotene** (PubChem IDs: 5280489) | −10.05 | 43.27 nM | LYS90, MET735, SER733, GLN86 |
| | | | α-glucan (PubChem IDs: _134692111) | −6.12 | 32.45 µM | **THR726***, **ASP725***, **GLN86***, **GLU89***, PHE82, LYS90, LEU93, MET94, GLU729 |
| 2 | IKK1/IKKA (PDB ID: 5EBZ) | Control ligand (inhibitor) | Parthenolide (PubChem IDs: 7251185) | −8.4 | 699.85 nM | **GLY22*, CYS98*, LEU21*,** VAL29, ILE164, VAL151, LYS44, ASN149, ASP165, GLY22, CYS98, ALA4, ASN149, ASP165, GLY22, CYS98, ALA42 |
| | | Test ligand (*S. platensis* bioactive compound) | **Phycocyanobilin** (PubChem IDs: _6438349) | −7.52 | 3.1 µM | **ARG20*, THR23*, GLU19*,** LEU21, VAL 151, GLY101, ILE164, ASN149, CYS98, LYS44 |
| | | | β-caroten (PubChem IDs: _5280489) | −7.08 | 6.45 µM | VAL29, VAL151, LEU21, MET95, ILE164, TYR97 |
| | | | α-glucan (PubChem IDs: _134692111) | −4.84 | 281.59 µM | **ARG20*, GLY22*, THR23*, GLU148*, CYS98*,** ASN28, GLY101, VAL151 |
| 3 | IKK2/IKKB (PDB ID:4KIK) | Control ligand (inhibitor) | Parthenolide (PubChem IDs: _7251185) | −8.03 | 1.29 µM | **CYS99*,** VAL29, VAL152, ILE165, LYS44, MET96, ASP166, LEU21, GLY22, VAL74, ALA42 |
| | | Test ligand (*S. platensis* bioactive compound) | **Phycocyanobilin** (PubChem IDs: _6438349) | −11.08 | 7.6 nM | **CYS99*, LYS106*, LEU21*, ASP103*, GLY22*, GLN100*,** VAL74, CYS99, VAL152, ILE165, VAL29, MET96, LYS106, GLU97, ALA42, GLY102, GLN110 |
| | | | β-Carotene (PubChem IDs: _5280489) | −6.43 | 19.32 µM | LYS106, ARG105, ARG47, PHE26, TRP58, GLU61, CYS46, GLN45, GLU149, ASP103, ASN109, GLN110 |
| | | | α-Glucan (PubChem IDs: _134692111) | −4.85 | 280.01 µM | **GLU97*, CYS99*, LEU21*, GLU149*, ASP103,** ALA42, VAL74, VAL29, LYS106, GLY102, VAL152 |

**Supplementary Table 1.** ***Continue***

| No | Protein | Ligand | Active Compound | ΔG (kcal/mol) | pKi | Binding Residues |
|---|---|---|---|---|---|---|
| 4 | NIK (PDB ID: 4IDV) | Control ligand (inhibitor) | Parthenolide (PubChem IDs: _7251185) | −7.46 | 3.41 µM | **ARG416*, LEU472*,** ARG408, VAL416, ALA427, LEU522, VAL414, VAL471, MET469, GLY475, GLU473 |
| | | Test ligand (*S. platensis* bioactive compound) | **Phycocyanobilin** (PubChem IDs: _6438349) | −10.96 | 9.23 nM | **ARG408*, SER410*, ARG416*, ARG666*,** ASP519 GLY409, LEU522, ARG405, GLU483, GLU473, LEU471, SER476, VAL414 |
| | | | β-Carotene (PubChem IDs: 5280489) | −5.15 | 169.06 µM | ARG408, LYS429, CYS444, ILE467, MET469, CYS533, LEU522, LEU472, VAL 414, VAL453, LEU455, PHE535, GLU440, GLY475, GLU470, ASP534, LEU441 |
| | | | α-Glucan (PubChem IDs: 134692111) | −5.14 | 169.66 µM | **LEU406*, ARG416*, GLN479*, ASP519*, ASN520*, LEU472*** |
| 5 | IκBα-NF-κB Complex (PDB ID: 1IKN) | Control ligand (inhibitor) | BAY-11-7082 ((E)-3-Tosylacrylonitrile) (PubChem IDs: 5353431) | −8.1 | 1.15 µM | **HIS245*, ARG246*, ASP290*,** LYS221, VAL244, VAL251 |
| | | Test ligand (*S. platensis* bioactive compound) | **Phycocyanobilin** (PubChem IDs: _6438349) | −7.62 | 2.58 µM | **LYS221***, **GLU286***, **PRO281***, **GLU222***, **ALA242***, SER288, ARG246, PRO182, MET279, HIS181, PHE184, PHE307, GLU284, VAL244, TYR251, LEU280, GLN289, ARG30, ARG15 |
| | | | β-Carotene (PubChem IDs: _5280489) | −3.82 | 1.58 mM | LYS221, LYS249, VAL251, PRO281, HIS245, TTYR289, VAL244, ARG246, ASP271, TYR248, GLU341 |
| | | | α-Glucan (PubChem IDs: _134692111) | −6.71 | 12.11 mM | **ARG246*, SER283*, GLU287*, VAL244*, SER288*, GLN249*, ALA242*,** GLN241,ALA242, HIS245, TYR251, GLU284 |
| 6 | NF-κB p65/p50 (PDB ID: 1VKX) | Control ligand (inhibitor) | Parthenolide (PubChem IDs: 7251185) | −6.29 | 24.69 µM | **LYS195***, **ILE196*,** CYS197, MET284, SER281 |
| | | Test ligand (*S. platensis* bioactive compound) | Phycocyanobilin (PubChem IDs: _6438349) | −6.77 | 10.86 µM | **ARG33***, **ARG605***, **ARG606***, LYS195, ARG35, ARG187, ASP217 |
| | | | **β-Carotene** (PubChem IDs: _5280489) | −8.64 | 463.53 nM | LEU154, ARG187, ALA188, LYS218, CYS120, ARG605, LYS575, VAL603, PHE34, TYR36, HIS88, HIS604, PRO600, ARG33, ASP185 |
| | | | α-Glucan (PubChem IDs: _134692111) | −2.18 | 25.1 mM | **ARG605***, **VAL603***, **LYS195***, **ASP217*,** PRO600 |

**Supplementary Table 1.** ***Continue***

| No | Protein | Ligand | **Active Compound** | ΔG (kcal/mol) | pKi | **Binding Residues** |
|---|---|---|---|---|---|---|
| 7 | COX-2 (PDB ID:5KIR) | Control ligand (inhibitor) | Celecoxib (PubChem IDs: 2662) | −11.01 | 8.51 nM | **ARG513***, **PHE518***, **LEU352***, **SER353***, **GLN192***, **HIS90***, VAL523, PHE518, TYR355, TRP387, VAL349, ALA527, ILE517, SER530, GLY526, ALA516, ARG120 |
| | | Control ligand (inhibitor) | Rofecoxib (PubChem IDs: 5090) | −10.15 | 36.35 nM | **ILE517*, PHE518*, HIS90*, ARG513*, ALA527***, VAL523, PHE518, LEU352, SER530, LEU531, VAL349, MET522, GLN192, ALA516 ARG120, SER353, GLY526, MET522, TYR355, SER530, LEU93, VAL116, |
| | | Test ligand (*S. platensis* bioactive compound) | Phycocyanobilin (PubChem IDs: 6438349) | −5.38 | 113.94 µM | MET113,VAL523, PHE205, TYR355, PHE357, PHE381, TYR385, VAL349, ALA527, VAL344, LEU534, GLY526, LEU384, LEU352, TRP387, LEU351, PHE518, TYP348, GLY533 |
| | | | β-Carotene (PubChem IDs: _5280489) | −5.98 | 41.16 µM | PRO514, ARG513, ILE564, HIS90, TYR91, HIS95, HIS351, ASP347, PHE580, HIS356, GLN192, GLY354, THR94 |
| | | | **α-Glucan** (PubChem IDs: 134692111) | −6.93 | 8.29 µM | **ARG513*, PHE518*, TYR355*, SER530*, MET522*, SER353*, GLN192***, VAL523, GLY526, LEU352, ALA527, TRP387, LEU93, VAL349, ALA516, ILE517 |

ΔG (mean binding energy); pKi (binding affinity); bold black markings: the bioactive compound of *S. platensis* with the best affinity; * and black bold: amino acid residues involved in hydrogen binding.

**Supplementary Table 2. Protein–Protein Interaction: NEMO (IKBKG), IKK1/IKKA (CHUK), IKK2/IKKB (IKBKB), NIK (MAP4K4), IκBα-NFκB Complex (NFKBIA), NF-κB p65 (RELA), NF-κB p50 (NFKB1), COX-2 (PTGS2)**

| No | #node1 | node2 | combined_score |
|---|---|---|---|
| 1 | CHUK | NFKBIA | 0.999 |
| 2 | CHUK | NFKB1 | 0.999 |
| 3 | CHUK | IKBKG | 0.999 |
| 4 | IKBKB | NFKBIA | 0.999 |
| 5 | IKBKB | NFKB1 | 0.999 |
| 6 | IKBKB | IKBKG | 0.999 |
| 7 | IKBKG | NFKBIA | 0.999 |
| 8 | NFKB1 | NFKBIA | 0.999 |
| 9 | NFKB1 | RELA | 0.999 |
| 10 | NFKBIA | RELA | 0.999 |
| 11 | CHUK | RELA | 0.998 |
| 12 | IKBKB | RELA | 0.998 |
| 13 | CHUK | IKBKB | 0.992 |
| 14 | IKBKG | RELA | 0.985 |
| 15 | IKBKG | NFKB1 | 0.982 |
| 16 | CHUK | MAP4K4 | 0.922 |
| 17 | IKBKB | MAP4K4 | 0.911 |
| 18 | IKBKG | MAP4K4 | 0.907 |
| 19 | NFKBIA | PTGS2 | 0.795 |
| 20 | IKBKB | PTGS2 | 0.62 |
| 21 | NFKB1 | PTGS2 | 0.603 |
| 22 | CHUK | PTGS2 | 0.589 |
| 23 | PTGS2 | RELA | 0.569 |